Classical and quantum regimes of the inhomogeneous Dicke model and its Ehrenfest time

Oleksandr Tsyplyatyev and Daniel Loss
Department of Physics, University of Basel, Klingelbergstraße 82, CH-4056 Basel, Switzerland
(Received 20 February 2010; revised manuscript received 28 June 2010; published 27 July 2010)

We show that in the few-excitation regime, the classical and quantum time evolution of the inhomogeneous Dicke model for N two-level systems coupled to a single boson mode agree for $N \gg 1$. In the presence of a single excitation only, the leading term in an $1/N$ expansion of the classical equations of motion reproduces the result of the Schrödinger equation. For a small number of excitations, the numerical solutions of the classical and quantum problems become equal for N sufficiently large. By solving the Schrödinger equation exactly for two excitations and a particular inhomogeneity, we obtain $1/N$ corrections which lead to a significant difference between the classical and quantum solutions at a new time scale which we identify as an Ehrenfest time, given by $\tau_E = \sqrt{N/\langle g^2 \rangle}$, where $\sqrt{\langle g^2 \rangle}$ is an effective coupling strength between the two-level systems and the boson.

DOI: 10.1103/PhysRevB.82.024305 PACS number(s): 42.50.Pq, 78.30.Ly

I. INTRODUCTION

The recent experimental advances on cold atoms in optical cavities,[1] Bose-Einstein condensation of exciton polaritons,[2] and observation of vacuum Rabi oscillations[3] in semiconductor microcavities renewed interest in light-matter interaction in the quantum coherent regime. These studies were motivated by an observation made by Dicke[4] long ago who realized that radiation from N identical two-level systems (spins 1/2) cannot be treated as a sum of N independent radiative processes but rather as a collective quantum phenomenon that involves all N spins and a photon mode even on the level of perturbation theory. Also, several schemes based on light-matter interaction to couple spatially separated spins that had been originally proposed as an element of a quantum computing device[5–8] were recently improved by a suggestion to use qubits constructed out of many spins to enhance coupling with the optical mode[9] due to the superradiant effect.

For instance, considerable attention was paid experimentally to the $\sqrt{N}$ enhancement of the light-matter coupling.[1,10] In typical setups, the spins are spatially separated, therefore the excitation energies of different spins may be different as they are affected by local forces that typically vary across the sample. The coupling strength to the light mode also varies as different spins are located at different positions of the mode due to a different amplitude of the electromagnetic field. Understanding of such inhomogeneities is important to find the practical limitations on the decoherence time of the system when, for instance, one designs a quantum computing device.[6,8,11] Also, the inhomogeneities are unavoidable and should be important in a system such as a semiconductor quantum-dot optical amplifier or laser.[12–14]

On the theoretical side, the homogeneous Dicke model, which describes a bath of N equivalent spins 1/2 with excitation (Zeeman) energy ϵ coupled to a quantized bosonic mode ω with the same coupling constants g, was diagonalized exactly in Ref. 15. The influence of inhomogeneities of the coupling constants g_j and Zeeman energies ϵ_j on the single-excitation dynamics was analyzed exactly in Refs. 16 and 17. It was shown that the boson occupation oscillates in time with a single Rabi frequency $\Omega = \sqrt{N\langle g^2 \rangle}$, where $\sqrt{\langle g^2 \rangle}$ is an effective coupling when only the coupling constants g_j are inhomogeneous but with constant Zeeman energies. If the Zeeman energies ϵ_j are also inhomogeneous but spread narrower than the threshold given by Ω this single frequency acquires a small Lamb-type shift whereas for a spread exceeding Ω, the boson decays completely in time.

In this paper, we show that the solution to the classical Hamilton equations of motion matches the solution of the time-dependent Schrödinger equation when the number of spins is large, i.e., $N \gg 1$ while the number of excitations p is still small, i.e., $p \ll N$. For a single excitation ($p=1$), the leading order in an $1/N$ expansion of the classical equations agrees with the quantum one. For a few excitations, such correspondence does not hold but for $p=2,3$, the numerical solutions of both classical equations of motion and Schrödinger equation agree for $N \gg 1$. It is plausible to assume that in leading $1/N$ order, the same correspondence holds for $p>3$. The numerical treatment of the Schrödinger equation with a large number of spins is possible since the Fock-space scales only as a power of $N(N^2, N^3, \ldots)$ in the few-excitation subspaces.

As the classical equations of motion for $p>1$ can also be mapped on the Schrödinger equation in the single-excitation subspace in leading $1/N$ order, the already available quantum result can be used to analyze the classical equations of motion for few excitations ($p \ll N$). For p excitations with $p>1$, we obtain the dynamics by simply rescaling the solution derived in Ref. 17 by p. This extends the single-excitation quantum solution to the case of few excitations when $N \gg 1$.

To assess the validity of the classical approximation for $p>1$ excitations, we solve the Schrödinger equation exactly in the two-excitation subspace with inhomogeneity in the coupling constants only and compare it with the classical solution. When N is small, both solutions are completely different. For large N, we perform an $1/N$ expansion of the quantum solution and recover the classical result in leading order. Subleading $1/N$ corrections cause deviations between quantum and classical dynamics which become significant at a large time scale $\tau_E = \sqrt{N/\langle g^2 \rangle}$ for $p \ll N$. We refer to this

time scale as an Ehrenfest time, defined here as the time where the quantum dynamics starts to differ from the classical dynamics.

Also, having found a quantum solution for $p=2$, we study it separately and, in particular, compare it with the $p=1$ quantum dynamics. We find that inhomogeneity of the coupling constants results in a different spectrum when N is finite: in the subspace with $p=1$, there is only one harmonic mode with a single frequency in the time-dependent occupation number of the boson, and for $p=2$, there are N discrete harmonic modes that form a continuum spectrum in the limit of large N. Such a mechanism can lead to destructive interference, thus to decay, of the excitations caused solely by the inhomogeneity of the coupling constants when $p>1$. But, as pointed out already, for $p=2$ we find that the leading $1/N$ term recovers the single-frequency dynamics in accordance with the classical solution. The decay due to inhomogeneous coupling constants thus manifests itself only in the first subleading $1/N$ correction. We find that this contribution is an oscillatory mode with frequency $\frac{3}{2}\Omega$ and a slowly decaying envelope. The decay behavior is essentially nonexponential with a long power-law tail and the decay time is $\tau_g \sim \sqrt{N/\langle g^2\rangle}$, where $\sqrt{\langle g^2\rangle}$ is a characteristic coupling. This decay occurs on the same time scale as the Ehrenfest time τ_E defined above. Thus, it can be described correctly only by the Schrödinger equation (and not by the classical one).

In our theoretical analysis, we assume the following ideal experiment. The spin bath is prepared in the ground state, e.g., dynamically or by the thermal cooling. The nonequilibrium dynamics of the boson is then initialized by a short radiation pulse from an external source which populates the boson mode with a few excitations like in Refs. 18–20 The dissipation of the boson mode, e.g., leakage of the photons through the mirrors that define an optical cavity can be used to detect the dynamics, similarly to the measurements performed on semiconductor quantum-well microcavities,[2,3,21] for the limiting case where the cavity leakage time exceeds the internal time scale.

The rest of the paper is organized as follows. In Sec. II, we discuss general properties of the inhomogeneous Dicke model. In Sec. III, we quote the already known solution to the Schrödinger equation in the single-excitation subspace. In Sec. IV, we construct the classical analog of the inhomogeneous Dicke model. Section V contains the exact solution of the Schrödinger equation in the two-excitation subspace for the inhomogeneous couplings only. In Sec. VI, we compare the numerical solution of the classical and the quantum equations of motions for two and three excitations in the limit of many spins. Section VII contains a discussion of applicability of the classical approximation. In the Appendix, we give some details on the calculation of the $1/N$ correction.

II. INHOMOGENEOUS DICKE MODEL

The Hamiltonian for the Dicke model that describes the interaction between a set of N spins 1/2 with excitation energies ϵ_j and a single bosonic mode of frequency ω is given by

$$H = \omega b^\dagger b + \sum_{j=1}^{N} \epsilon_j S_j^z + \sum_{j=1}^{N} g_j (S_j^+ b + S_j^- b^\dagger), \tag{1}$$

where $S_j^\pm = S_j^x \pm i S_j^y$, S_j^z are spin 1/2 operators, and $b(b^\dagger)$ are the standard Bose annihilation (creation) operators. The coupling constants g_j are typically given as dipole matrix elements and thus are, in general, complex numbers. Since their phases can be eliminated by a unitary transformation, we treat g_j as real and positive numbers.

In the present paper, we assume that the boson mode is tuned in resonance with the spins $\langle \epsilon_j \rangle = \omega$, where $\langle \cdots \rangle = \Sigma_j \cdots / N$. If the boson mode is strongly detuned, $|\langle \epsilon_j \rangle - \omega| \gg \sqrt{\langle g^2 \rangle}$, the interaction between them is weak and the model Eq. (1) can be analyzed perturbatively.[11] Also note that the inhomogeneities of g_j and/or ϵ_j forbids to represent the Hamiltonian Eq. (1) in terms of the total angular momentum operators $J_\alpha = \Sigma_j S_j^\alpha$, $\alpha = x, y, z$.

The total number of spin-boson excitations, $L = n + \Sigma_j S_j^z$, is conserved by the model Eq. (1), where $n = b^\dagger b$ is the bosonic occupation number. The eigenvalue c of L labels the subspace of the Hamiltonian with a given total number of excitations.

We restrict ourselves to a small number of excitations, $p \ll N$. In the following, we assume that the spins can be prepared in the ground state with each spin in its low Zeeman state. The bosonic mode is assumed to be occupied by p bosons initially, the time evolution is restricted to the subspace with $c = -N/2 + p$. Then the leakage of the boson mode to the outside world can be used to monitor the time dynamics of the system by detecting the leaked mode at given subsequent instances in time.

III. SINGLE EXCITATION

The time dynamics of Eq. (1) for a single excitation was analyzed in detail in Ref. 17. Here we only quote the explicit form of the corresponding Schrödinger equation and the main results derived from it.

The time evolution is restricted the subspace with $c = -N/2 + 1$ and is described by the general state,

$$|\Psi(t)\rangle = \alpha(t)|\Downarrow, 1\rangle + \sum_{j=1}^{N} \beta_j(t)|\Downarrow\uparrow_j, 0\rangle, \tag{2}$$

where $\alpha(t)$ and $\beta_j(t)$ are normalized amplitudes, $|\alpha(t)|^2 + \Sigma_j |\beta_j(t)|^2 = 1$, of finding either a state with one boson and no spin excitations present or a state with no boson and the jth spin excited (flipped). As initial condition, we will assume throughout (with one exception discussed at the end) that initially only bosonic excitations are present while each spin is in its individual ground state, i.e., $\alpha(t=0) = 1$. The state $|\Psi(t)\rangle$ from Eq. (2) describes then the time evolution of an initial product state $|\Downarrow, 1\rangle$ into an entangled state formed by a coherent superposition of $N+1$ states, where each $|\Downarrow\uparrow_j, 0\rangle$ contains an excited spin and no boson. This entangled state can be viewed as a (para) magnon state in the uniform limit. In other words, the initial bosonic excitation gets coherently spread out over the entire system in course of time.

Inserting $|\Psi(t)\rangle$ from Eq. (2) into the time-dependent Schrödinger equation, we get

$$-i\dot{\alpha}(t) = \sum_j g_j \beta_j(t),$$

$$-i\dot{\beta}_k(t) = (\epsilon_j - \omega)\beta_k(t) + g_k \alpha(t). \tag{3}$$

This set of coupled equations can be solved explicitly via Laplace transformation. We use the same approach to solve the Schrödinger equation in the two-excitation subspace in Sec. V of this paper.

If the number of spins is large, $N \gg 1$, the sum over j in the exact solution of Eq. (3) can be substituted by an integral. In this continuum limit, the discrete set of ϵ_j and g_j become continuous variables characterized by distribution functions $Q(g)$ and $P(\epsilon)$. Any distribution function of g results only in a renormalized coupling constant $\sqrt{\langle g^2 \rangle}$ and the dynamics of the boson is not affected in any other way.

Different distribution functions of ϵ result in qualitatively different regimes of the dynamics. Let us choose $P(\epsilon)$ as a rectangular pulse shape of width Δ centered around ω,

$$P(\epsilon) = \theta(-\epsilon + \omega + \Delta/2)\,\theta(\epsilon - \omega + \Delta/2), \tag{4}$$

where $\theta(x)$ is the Heaviside step function. It was shown that when the inhomogeneity is below a certain threshold, $\Delta/\Omega \ll 1$, where $\Omega = \sqrt{N\langle g^2 \rangle}$ is the collective Rabi frequency, the boson excitation, $\langle n \rangle = |\alpha(t)|^2$, does not decay, i.e.,

$$\langle n(t) \rangle = \cos^2(\Omega t). \tag{5}$$

The corrections to this result are small and are on the order of Δ/Ω. In the opposite limit, $\Delta/\Omega \gg 1$, the spins act as the thermal bath at zero temperature. The bosonic excitation decays completely and exponentially,

$$\langle n(t) \rangle = \exp(-t/t_2) \tag{6}$$

with the decay time $t_2 = 2\Delta/\pi\Omega^2$. In the intermediate regime, $\Delta \simeq \Omega$, the decay is partial and the decay law is a combination of exponential and inverse-power laws.

IV. CLASSICAL APPROXIMATION

To construct classical equations, we use approach of Refs. 22 and 23. As a result, the Hamilton equations of motion for the model Eq. (1) are

$$\dot{a} = -i\sum_j g_j C_j^-, \tag{7}$$

$$\dot{C}_j^- = -i(\epsilon_j - \omega)C_j^- - i g_j a, \tag{8}$$

where $C_j^- = C_j^x - iC_j^y$ are the in-plane components of the classical spins and a is a classical complex variable. These differential equations can be solved with the initial conditions $C_j^-(0) = 0$ and $a(0) = \sqrt{p}$ to obtain the time-dependent value of the bosonic field $n(t) = |a(t)|^2$.

In the above, equation for the spins, Eq. (8), is also approximated for a small number of excitations $p \ll N$ assuming that z components of all spins stay at the initial values at all times $C_j^z(t) \approx -1/2$. The quantity $L = |a^2| + \Sigma_j C_j^z$ is conserved during the evolution governed by the model Eq. (1). Thus, at any instance of time $\Sigma_j C_j^z \approx -N/2$, i.e., when the dynamics starts with only a few bosonic excitations, the spins cannot "flip" during the evolution and equation for $C_j^z(t)$ drops out from the complete set of equations of motion.

When $p=1$, the Hamilton Eqs. (7) and (8) coincide formally with the Schrödinger Eq. (3). By direct comparison, we can establish the correspondence between the quantum-mechanical amplitudes and the classical variables: the classical field a is the amplitude α and the in-plane component of the spin vector C_j^- is the amplitude β_j. Note that the classical spins are not averages of the spin operators, $\langle \mathbf{S}_j \rangle \equiv 0$ but instead they are connected with the quantum-mechanical amplitudes. The solution of the dynamical Eqs. (7) and (8) is the same as the solution of Eq. (3).

V. TWO-EXCITATION REGIME AND INHOMOGENEOUS COUPLING CONSTANTS

In this section, we consider the dynamics of two excitations for a system with inhomogeneous coupling constants g_j but constant Zeeman energies $\epsilon_j = \omega$.

The time evolution of the two excitations is restricted to the subspace with $c = -N/2 + 2$ and is described by the general state,

$$|\Psi(t)\rangle = \alpha(t)|2, \Downarrow\rangle + \sum_j \beta_j |1, \Downarrow \uparrow_j\rangle + \sum_{i>j} \gamma_{ij} |0, \Downarrow \uparrow_i \uparrow_j\rangle, \tag{9}$$

where $\alpha(t)$, $\beta_j(t)$, and $\gamma_{ij}(t)$ are the normalized amplitudes, $|\alpha(t)|^2 + \Sigma_j |\beta_j(t)|^2 + \Sigma_{i>j} |\gamma_{ij}|^2 = 1$, of the state with two bosonic excitations, a state with one bosonic excitation and the jth spin excited, and a state with no bosonic excitation and the ith and jth spins excited (with $i \neq j$). The amplitude γ_{ij} is defined such that $\gamma_{ij} = 0$ if $j \geq i$.

The conservation law can be used to simplify the Hamiltonian Eq. (1). We subtract ωL from Eq. (1), which only changes an irrelevant overall phase of $|\Psi(t)\rangle$, to eliminate the first two terms. Note that the second term will not be zero away from the resonance $\omega \neq \epsilon$. Inserting $|\Psi(t)\rangle$ into the time-dependent Schrödinger equation we then obtain

$$-i\dot{\alpha}(t) = \sqrt{2}\sum_j g_j \beta_j(t),$$

$$-i\dot{\beta}_k(t) = \sqrt{2} g_k \alpha(t) + \sum_{j<k} g_j \gamma_{kj}(t) + \sum_{j>k} g_j \gamma_{jk}(t),$$

$$-i\dot{\gamma}_{kl}(t) = [g_k \beta_l(t) + g_l \beta_k(t)](1 - \delta_{kl}). \tag{10}$$

The initial condition, $\alpha(0) = 1$ and $\beta_j(0) = \gamma_{ij}(0) = 0$, which we further assume corresponds to the doubly occupied boson mode at the initial time. The physical observable of interest is the time-dependent value of the boson occupation number $\langle n(t) \rangle$, which can be expressed in terms of the amplitudes $\alpha(t)$ and $\beta_j(t)$ as

$$\langle n(t)\rangle = 2|\alpha(t)|^2 + \sum_j |\beta_j(t)|^2, \tag{11}$$

where $\langle\cdots\rangle = \langle\Psi(t)|\cdots|\Psi(t)\rangle$ is the time-dependent expectation value.

A. General solution

We use the Laplace transform, $A(s)=\int_0^\infty dt A(t)e^{st}$, to solve the set of equations, Eq. (10). In the Laplace domain, Eq. (10) is a set of linear algebraic equations,

$$-i(s\alpha - 1) = \sqrt{2}\sum_j g_j\beta_j,$$

$$-is\beta_k = \sqrt{2}g_k\alpha + \sum_{j<k} g_j\gamma_{kj} + \sum_{j>k} g_j\gamma_{jk},$$

$$-is\gamma_{kl} = (g_k\beta_l + g_l\beta_k)(1-\delta_{kl}), \tag{12}$$

that can be explicitly solved. The substitution of $\alpha(s)$ and $\gamma_{kl}(s)$ as functions of $\beta_k(s)$, that are obtained from the first and the last lines, into the middle line gives the following set of equations for β_k only:

$$\left(-s^2 + 2g_k^2 - \sum_j g_j^2\right)\frac{\beta_k}{g_k} = 3\sum_j g_j\beta_j - i\sqrt{2}. \tag{13}$$

Each $\beta_k(s)$ is easily found from the above equation since $\Sigma_j g_j\beta_j(s)$ on the right-hand side is the same in each equation for all $\beta_k(s)$. Then the sum is found self-consistently and we obtain the solution for the amplitude as

$$\beta_k(s) = \frac{-i\sqrt{2}g_k}{-s^2 + 2g_k^2 - N\langle g^2\rangle}\frac{1}{1-3\left\langle\frac{g_j^2 N}{-s^2+2g_j^2-N\langle g^2\rangle}\right\rangle}, \tag{14}$$

where the average is the sum over all spins $\langle\cdots\rangle = (\Sigma_j\cdots)/N$. The other two amplitudes are found from the first and the third lines of Eq. (12) by substitution of the above solution for $\beta_k(s)$,

$$\alpha(s) = \frac{1}{s}\frac{1-\left\langle\frac{g_j^2 N}{-s^2+2g_j^2-N\langle g^2\rangle}\right\rangle}{1-3\left\langle\frac{g_j^2 N}{-s^2+2g_j^2-N\langle g^2\rangle}\right\rangle}, \tag{15}$$

$$\gamma_{kl}(s) = \frac{i}{s}(g_k\beta_l + g_l\beta_k)(1-\delta_{kl}). \tag{16}$$

The main focus of our interest will be on Eqs. (14) and (15) as the observable quantity $\langle n(t)\rangle$ depends only on $\alpha(t)$ and $\beta_k(t)$. These time-dependent amplitudes can be obtained from Eqs. (14) and (15) by the inverse Laplace transform. The analytic structure of Eqs. (14) and (15) is governed, in general, by a set of poles given by the roots of denominators which depend on a particular set of g_j. For instance, if the number of spins N is small, there are $2N$ conjugated complex roots. The inverse Laplace transforms of $\alpha(s)$ and $\beta_k(s)$ will be a sum of N discrete harmonic modes in contrast to the single-excitation dynamics where in such a setup there is just a single pair of roots independent of the particular set of g_j, see Sec. III, and there is only a single harmonic mode in the dynamics of the boson occupation number, see Eq. (5). Such a result marks a qualitative difference in the dynamics of the single- and two-excitation subspaces.

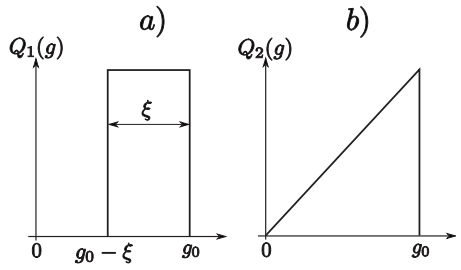

FIG. 1. Distribution functions of g that are used to evaluate the sums in Eqs. (14) and (15). (a) The uniform distribution function $Q_1(g)$ has a maximum coupling strength g_0 and a width ξ which can vary from 0 (i.e., homogeneous coupling constants) to g_0 (i.e., maximally inhomogeneous coupling constants). (b) The sawtooth distribution function $Q_2(g)$ describes a nonuniform spread of the coupling constants g_j from 0 to g_0.

B. Time evolution in the continuum limit of many spins

In this section, we study the limit of many spins, i.e., $N \gg 1$. The sum over j in Eqs. (14) and (15) can be substituted by an integral over a distribution function of g, $\Sigma_j\cdots \to N\int_0^\infty dg Q(g)\ldots$ In the continuum limit, some poles can merge together, forming branch cuts, and some poles can separate themselves from the others. The inverse Laplace transform of the branch cuts will become a decay function in the time domain and the separate poles will contribute a set of harmonic modes. The analytic structure of $\alpha(s)$ and $\beta_k(s)$ explicitly depends on the particular form of $Q(g)$.

C. Uniform distribution function

To be specific, we consider a set of coupling constants which are uniformly distributed from a minimum value $g=g_0-\xi$ to a maximum value $g=g_0$,

$$Q_1(g) = \theta(-g+g_0)\theta(g-g_0+\xi)/\xi. \tag{17}$$

The coupling constants cannot be negative so ξ can vary from $\xi=0$ (e.g., all couplings are the same and are equal to g_0) to $\xi=g_0$ (e.g., the couplings are evenly distributed from 0 to g_0), see Fig. 1(a). A useful property of this distribution function Q_1 is that a small and a large inhomogeneity can be analyzed on the same footing. Another distribution function will be considered in the next section.

Turning the sum in Eqs. (14) and (15) into an integral and using $Q_1(g)$, we obtain

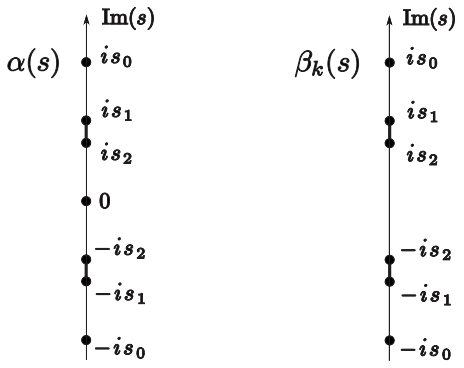

FIG. 2. Analytic structure of the time-dependent quantum-mechanical amplitudes for $p=2$ excitations in the Laplace domain, Eqs. (14) and (15), in the continuum approximation calculated using the distribution functions $Q_1(g)$ and $Q_2(g)$. Separated dots, $0, \pm is_0$, are poles and the dots, $\pm is_{1,2}$, connected by bold lines, are branch points. The bold lines are the corresponding branch cuts.

$$\left\langle \frac{g_j^2 N}{-s^2+2g_j^2-N\langle g^2\rangle} \right\rangle = -\frac{N}{2}\left\{ \frac{\sqrt{-s^2-N\langle g^2\rangle}}{\sqrt{2}\xi} \arctan\left[\frac{\sqrt{2}\xi\sqrt{-s^2-N\langle g^2\rangle}}{s^2+N\langle g^2\rangle-2g_0(g_0-\xi)} \right] + 1 \right\} \tag{18}$$

where $\langle g^2\rangle = g_0^2 - \xi g_0 + \xi^2/3$.

The analytic structure of $\alpha(s)$ from Eq. (15) with the sum from Eq. (18) is the following. There are three poles and two branch cuts, see Fig. 2. Thus, the inverse Laplace transform has two contributions $\alpha(t)=\alpha_p(t)+\alpha_c(t)$. One pole is at $s=0$ and two poles are at $s=\pm is_0$, where $s_0=2\sqrt{N\langle g^2\rangle}$. These are given by zeroes of the denominator of the second term in the product in Eq. (15). Note that s_0 was obtained using a $1/N$ expansion and is independent of ξ in leading order. In the first subleading $1/N$ order, s_0 depends on ξ,

$$s_0 = 2\sqrt{N\langle g^2\rangle - \frac{3}{10}g_0^2}, \tag{19}$$

when $\xi=g_0$ and

$$s_0 = 2\sqrt{N\langle g^2\rangle - \frac{1}{2}g_0^2}, \tag{20}$$

when $\xi=0$. The inverse Laplace transform of the functions with poles is a sum over the corresponding residues, $\alpha_p(t) = \Sigma_{s=0,\pm is_0} \mathrm{Res}_s\, \alpha(s)e^{st}$, and it gives

$$\alpha_p(t) = \frac{1}{2} + \frac{1}{2}\cos s_0 t + \frac{1}{N}\delta\alpha(\xi). \tag{21}$$

Here, the leading term is independent of ξ unlike the first $1/N$ correction, $\delta\alpha(g_0) = -\frac{27}{20}[1-\cos(s_0 t)]$ and $\delta\alpha(0) = -[\frac{1}{4} - \frac{1}{2}\cos(s_0 t)]$. We refer to Appendix for the calculation.

The expression in Eq. (18) has four branch points. Two are given by the square root, $s=\pm is_1$, where $s_1=\sqrt{N\langle g^2\rangle}$. The remaining two are given by arctan. Solving the equation,

$$\frac{\sqrt{2}\xi\sqrt{-s^2-N\langle g^2\rangle}}{s^2+N\langle g^2\rangle-2g_0(g_0-\xi)} = \pm i \tag{22}$$

we find them as $s=\pm is_2$, where $s_2 = \sqrt{N\langle g^2\rangle - \xi^2 - 2g_0(g_0-\xi) - \xi\sqrt{\xi^2+4g_0(g_0-\xi)}}$. The first branch cut is chosen as a straight line between is_1 and is_2 and the second branch cut as a straight line between $-is_2$ and $-is_1$, see Fig. 2.

The contribution to the inverse Laplace transform from the branch cuts is a function of ξ. When $\xi=0$, Eq. (18) has no branch points. In the $\xi\to 0$ limit, the arctan can be expanded in the small parameter, then the leading term is nonzero and contains no multivalued functions. All the higher-order terms are proportional to ξ and are zero when $\xi=0$. We obtain in this limit $\alpha_c(t)=0$.

When $\xi=g_0$, the integral enclosing the branch cuts,

$$\alpha_c(t) = \frac{32}{3N^2}\int_0^1 dx \frac{x^2\cos(\sqrt{s_1^2-2g_0^2x^2}\,t)}{\left[\frac{x}{2}\ln\left(\frac{1+x}{1-x}\right)-1\right]^2+\left(\frac{\pi}{2}x\right)^2}, \tag{23}$$

contributes only to the second subleading $1/N$ order of $\alpha(t)$. Thus, $\alpha_c(t)$ is beyond the accuracy of the present calculation for all values of ξ and it can be neglected compared to the leading-order correction in Eq. (21).

The analytic structure of $\beta_k(s)$ in Eq. (14) is the same as $\alpha(s)$ except that there is no pole at $s=0$, see Fig. 2. Thus the inverse Laplace transform also has two contributions, $\beta_k(t)=\beta_k^p(t)+\beta_k^c(t)$, when $\xi>0$. One is given by the sum over just two residues, $s=\pm is_0$, instead of three, $\beta_k^p(t) = \Sigma_{s=\pm is_0}\mathrm{Res}_s\, \beta_k(s)e^{st}$, and yields

$$\beta_k^p(t) = \frac{-ig_k\sin(s_0 t)}{\sqrt{2N\langle g^2\rangle}} + \frac{1}{N}\delta\beta_k(\xi), \tag{24}$$

where, similarly to Eq. (21), only the first $1/N$ correction depends on ξ but the leading term does not, $\delta\beta_k(g_0) = -ig_k[2(g_k/g_0)^2-3]\sin(s_0 t)/\sqrt{2N\langle g^2\rangle}$ and $\delta\beta_k(0) = i\sin(s_0 t)/4\sqrt{2N}$, see Appendix for the calculation.

When $\xi=0$, the branch cuts disappear, $\beta_k^c(t)=0$, similarly to $\alpha_c(t)$. When $\xi=g_0$ the analysis of the branch cuts is a bit different from above for $\alpha_c(s)$. There is a singularity in Eq. (14) at $s=\pm i\sqrt{N\langle g^2\rangle - 2g_k^2}$, originating from the first term in the product in Eq. (14), which overlaps with the branch cuts. It present a difficulty if we apply continuum approximation to the discrete form of $\beta_k(s)$ in the same way as we did to $\alpha(s)$. Cancellation of this singularity by a zero in the denominator of the second term in the product in the original discrete form, Eq. (14), simplifies the analysis. The analytic structure of $\beta_k(s)$ in the continuum approximation does not alter. The only difference is a small $1/N$ correction to Eq. (18). Repeating the same steps as between Eqs. (18) and (23), we obtain the following expression for the integral enclosing the branch cuts:

$$\beta_k^c(t) = -\frac{2\sqrt{2}g_k^3 g_0^2}{3N\sqrt{N\langle g^2\rangle}}\int_0^1 dx \frac{x^2[2i\,\sin(\sqrt{N\langle g^2\rangle - 2g_0^2x^2}t)]}{\left\{\frac{2g_0^2x^2 - g_k^2}{1}\frac{2}{3N} + g_k^2\left[\frac{x}{2}\ln\left(\frac{1+x}{1-x}\right) - 1\right]\right\}^2 + \left[g_k^2\frac{\pi}{2}x\right]^2}. \tag{25}$$

Here, the integral can be simplified by performing an $1/N$ expansion. This approximation is valid for the majority of $g_k \gg 2g_0/3N$ except for a small set of $g_k \ll 2g_0/3N$, where the maximum value of $|\beta_k^c(t)| \leq \frac{\sqrt{2}}{6N^2}$ is small as $1/\sqrt{N}$ compared to the majority of $g_k \gg 2g_0/3N$. As a result, the leading $1/N$ term is

$$\beta_k^c(t) = -\frac{\sqrt{2}}{g_k}\frac{4ig_0^2}{3N\sqrt{N\langle g^2\rangle}}I(t), \tag{26}$$

where the dimensionless integral $I(t)$ describes the time decay,

$$I(t) = \int_0^1 dx \frac{x^2\,\sin(\sqrt{N\langle g^2\rangle - 2g_0^2x^2}t)}{\left[\frac{x}{2}\ln\left(\frac{1+x}{1-x}\right) - 1\right]^2 + \left(\frac{\pi}{2}x\right)^2} \tag{27}$$

and is independent of k. In contrast to $\alpha_c(t)$, $\beta_k^c(t)$ does contribute to the first subleading $1/N$ order of $\beta_k(t)$ and we will analyze it below.

The argument of the sine in Eq. (27) can be expanded in $1/N$, $\sqrt{N\langle g^2\rangle - 2g_0^2x^2} \approx \sqrt{N\langle g^2\rangle} - \frac{g_0^2x^2}{\sqrt{N\langle g^2\rangle}}$. The leading term $\sqrt{N\langle g^2\rangle}t$, which is a fast oscillating function, can be taken outside of the integral. The second term gives a slow decay envelope. This term leads to a significantly decay when $g_0^2t/\sqrt{N\langle g^2\rangle} = 1$. Thus, we estimate the decay time as

$$\tau_g = \sqrt{N/\langle g^2\rangle}, \tag{28}$$

see Fig. 3. At a large time $t \gg \sqrt{N/\langle g^2\rangle}$, $I(t)$ has a power-law tail. Due to fast oscillations of the sine, the main contribution to the integral comes from $x \ll \sqrt[4]{N\langle g^2\rangle}/\sqrt{g_0^2t}$, thus, the spectral function can be approximated as $x^2/\{[\frac{x}{2}\ln(\frac{1+x}{1-x}) - 1]^2 + (\frac{\pi}{2}x)^2\} \approx x^2$. Then, we also expand the argument of the sine in Eq. (27) as $\sqrt{N\langle g^2\rangle - 2g_0^2x^2} \approx \sqrt{N\langle g^2\rangle} - \frac{g_0^2x^2}{\sqrt{N\langle g^2\rangle}}$, the integral in Eq. (27) evaluates in terms of an error function which we expand, again, in a Taylor series in powers of $\sqrt{N\langle g^2\rangle}/g_0^2t \ll 1$, and obtain

$$I(t) = \frac{\chi}{2g_0t}\left\{\cos\left[\left(\chi - \frac{1}{\chi}\right)g_0t\right] - \frac{1}{2}\sqrt{\frac{\pi\chi}{2g_0t}}[\sin(\chi g_0t) + \cos(\chi g_0t)]\right\}, \tag{29}$$

where $\chi = \sqrt{N\langle g^2\rangle}/g_0$. The shape of the asymptote is in qualitative agreement with the explicit numerical evaluation of Eq. (27), however, the overall amplitude is different by a factor of 3, see Fig. 3, as we neglected the logarithmic singularity at $x=1$ in the initial integral.

In the sum of two amplitudes $\alpha(t)$ and $\beta_k(t)$, the decay shows up only in the fist subleading $1/N$ order when the number of spins is large. The particular form of the decay function is rather involved and is not displayed here.

The decay on the short time scale $t < \tau_g$ is essentially nonexponential, see Fig. 3. The particular shape depends on the particular set of the strongest coupling constants g_j. However, an estimate of the time scale $\tau_g \sim \sqrt{N/\langle g^2\rangle}$ is independent of $Q(g)$, as it is based on an $1/N$ expansion only, i.e., the distance between the branch points in Fig. 3 is smaller by $1/N$ compared to the distances between the branch points and the poles. The power-law tail exists due to a bound on the smallest g_j. The power and the numerical prefactor in Eq. (29) depend on a particular $Q(g)$, especially on the distribution of the smallest g_j's as they are responsible for the long-time behavior.

The time-dependent occupation number of the boson can also be expanded into a $1/N$ series. The leading term depends on ξ only through the effective coupling $\sqrt{\langle g^2\rangle}$,

$$\langle n(t)\rangle = 2\,\cos^2\left(\frac{s_0t}{2}\right) + \frac{1}{N}\delta n(t). \tag{30}$$

The leading $1/N$ correction, $\delta n(t) = 4\alpha(t)\delta\alpha(t) + 2\Sigma_j\beta_j(t)\delta\beta_j(t)$, is qualitatively different for $\xi = 0$ and $\xi > 0$. When the coupling constants are homogeneous, $\xi = 0$,

$$\delta n(t) = -\left\{2[1 + \cos(s_0t)] + \frac{1}{8}[1 - \cos(2s_0t)]\right\} \tag{31}$$

is an oscillatory function where the second harmonic with the doubled frequency $2s_0$ appears in addition to the main frequency s_0 of the leading term. For the case of maximally inhomogeneous coupling constants, $\xi = g_0$, the function

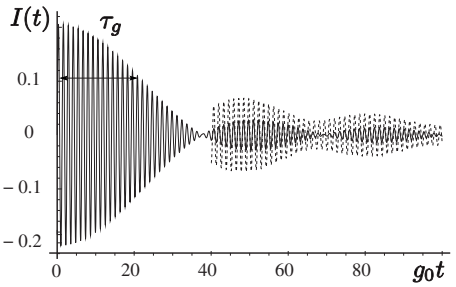

FIG. 3. Decay correction to the dynamics of the boson Eq. (27) for the parameter $\sqrt{N\langle g^2\rangle}/g_0 = 5$. The solid line is a numerical evaluation of the integral, where τ_g marks the time scale of the initial decay. The dashed line is the long-time asymptote Eq. (29).

$$\delta n(t) = 1.8\,\sin^2(s_0 t) - 2\,\sin(s_0 t) I(t) \tag{32}$$

contains a decaying contribution, where $I(t)$ is the decay function from Eq. (27). Up to the time scale τ_g, the term $\sin(s_0 t) I(t) \sim \sin(s_0 t)\cos(s_1 t)$ is a harmonic mode with the third frequency $s_0 + s_1$ in addition to s_0 and $2s_0$. This mode can only be observed if the short-time regime with $t < \tau_g$ is accessible to measurement.

D. Sawtooth distribution function $Q_2(g)$

Here we study another distribution of the coupling constants. Assuming that there are more spins at the nodes of the cavity mode so that the stronger coupling constants are more favorable, we consider a sawtoothlike distribution function with its maximum at the largest coupling strength g_0, $Q_2(g) = 2g/g_0^2 \theta(-g+g_0)\theta(g)$, see Fig. 1(b).

Replacing the sums in Eqs. (14) and (15) by integrals, $\Sigma_j \cdots \to N\int_0^\infty dg Q(g)\ldots$, and using $Q_2(g)$ we get

$$\left\langle \frac{g_j^2 N}{-s^2 + 2g_j^2 - N\langle g^2\rangle} \right\rangle = \frac{N}{2}\left[1 - \frac{s^2 + N\langle g^2\rangle}{2g_0^2} \ln\left(\frac{s^2 + N\langle g^2\rangle}{s^2 + N\langle g^2\rangle - 2g_0^2}\right)\right], \tag{33}$$

where $\langle g^2\rangle = g_0^2/2$.

The analytic structure of Eqs. (14) and (15) with the sum from the above equation is the same as with the sum from Eq. (18) obtained using $Q_1(g)$. There are three poles [$\alpha(s)$ has three poles and $\beta_k(s)$ has only two as in the previous section] and two branch cuts, see Fig. 2. Thus, the inverse Laplace transforms of $\alpha(s)$ and $\beta_k(s)$ also have two contributions, i.e., $\alpha(t) = \alpha_p(t) + \alpha_c(t)$ and $\beta_k(t) = \beta_k^p(t) + \beta_k^c(t)$. Similarly to the previous section, there is a pole at $s=0$ and there are two poles at $s = \pm i s_0$, where $s_0 = 2\sqrt{N\langle g^2\rangle}$ agrees in leading $1/N$ order with what was obtained in the previous section. The four branch points, which are due to the logarithm in Eq. (33), are found from

$$\frac{s^2 + N\langle g^2\rangle}{s^2 + N\langle g^2\rangle - 2g_0^2} = 0, \infty, \tag{34}$$

as $s = \pm i s_{1,2}$ where $s_1 = \sqrt{N\langle g^2\rangle}$ and $s_2 = \sqrt{N\langle g^2\rangle - 2g_0^2}$. These also agree with what we have already found in the previous section when the coupling constants were maximally inhomogeneous, i.e., $\xi = g_0$.

The sums over the residues give the main contribution to the inverse Laplace transforms. The leading $1/N$ terms in $\alpha(t)$ and $\beta_k(t)$ agree with the leading terms in Eqs. (21) and (24), where $\langle g^2\rangle$ has to be calculated using the sawtooth distribution function $Q_2(g)$ instead of $Q_1(g)$. The contributions from the branch cuts also appear only in the first subleading $1/N$ order. The main features of the time decay are similar to that of Eq. (27). Indeed, the decay time τ_g and the frequency of the fast oscillating term in Eq. (27) for times $t < \tau_g$ result from the same branch points, $\pm i s_{1,2}$, as in the previous section.

As the amplitudes $\alpha(t)$ and $\beta_k(t)$ are similar to the ones in the previous subsection, the boson number $\langle n(t)\rangle$ is also given by Eq. (30). The leading $1/N$ term depends on $Q_2(g)$ only through the effective coupling constant $\sqrt{\langle g^2\rangle}$, and the leading $1/N$ correction contains a decay term.

VI. SUBSPACE OF TWO AND THREE EXCITATIONS

In this section, we compare numerically the solution of the Schrödinger equation with the one of the classical equations of motion Eqs. (7) and (8) for $p=2,3$ excitations. We start from writing down the Schrödinger equation in these two subspaces explicitly.

The time evolution of two excitations is restricted to the subspace with $c = -N/2 + 2$ and is described by the general state Eq. (9). The Schrödinger equation for an arbitrary set of ϵ_j and g_j in this subspace is similar to Eq. (10),

$$\begin{aligned} -i\dot{\alpha} &= \sqrt{2}\sum_j g_j \beta_j, \\ -i\dot{\beta}_k &= (\epsilon_k - \omega)\beta_k + \sqrt{2} g_k \alpha + \sum_{j<k} g_j \gamma_{kj} + \sum_{j>k} g_j \gamma_{jk}, \\ -i\dot{\gamma}_{kl} &= [(\epsilon_k - \omega) + (\epsilon_l - \omega)]\gamma_{kl} + (g_k \beta_l + g_l \beta_k)(1 - \delta_{kl}) \end{aligned} \tag{35}$$

with the initial condition $\alpha(0)=1$, $\beta_k(0)=0$, and $\gamma_{kl}(0)=0$.

The subspace of three excitations is labeled by $c = -N/2 + 3$ and is described by the general state,

$$|\Psi(t)\rangle = \alpha(t)|3, \Downarrow\rangle + \sum_j \beta_j |2, \Downarrow \uparrow_j\rangle + \sum_{i>j} \gamma_{ij} |1, \Downarrow \uparrow_i \uparrow_j\rangle + \sum_{i>j>r} \eta_{rij} |0, \Downarrow \uparrow_r \uparrow_i \uparrow_j\rangle, \tag{36}$$

where $\alpha(t)$, $\beta_j(t)$, $\gamma_{ij}(t)$, and $\eta_{rij}(t)$ are the normalized amplitudes, $|\alpha(t)|^2 + \Sigma_j |\beta_j(t)|^2 + \Sigma_{i>j} |\gamma_{ij}|^2 + \Sigma_{i>j>r} |\eta_{rij}|^2 = 1$, of the state with three bosonic excitations, a state with two bosonic excitations and the jth spin excited, a state with one bosonic excitation and the ith and jth spins excited, and a state with no bosonic excitations and the ith, jth, and rth spins excited. The amplitude γ_{ij} is defined such that $\gamma_{ij}=0$ if $j \geq i$, and η_{rij} is defined such that $\eta_{rij}=0$ if the inequality $i>j>r$ is not satisfied. The Schrödinger equation in this subspace is

$$\begin{aligned} -i\dot{\alpha} &= \sqrt{3}\sum_j g_j \beta_j, \\ -i\dot{\beta}_k &= (\epsilon_k - \omega)\beta_k + \sqrt{3} g_k \alpha + \sqrt{2}\sum_{j<k} g_j \gamma_{kj} + \sqrt{2}\sum_{j>k} g_j \gamma_{jk}, \\ -i\dot{\gamma}_{kl} &= [(\epsilon_k - \omega) + (\epsilon_l - \omega)]\gamma_{kl} + \sqrt{2}(g_k \beta_l + g_l \beta_k)(1 - \delta_{kl}) + \sum_{j>k>l} g_j \eta_{jkl} + \sum_{k>j>l} g_j \eta_{kjl} + \sum_{k>l>j} g_j \eta_{klj}, \\ -i\dot{\eta}_{klm} &= [(\epsilon_k - \omega) + (\epsilon_l - \omega) + (\epsilon_m - \omega)]\gamma_{kl} + g_k \gamma_{lm} + g_l \gamma_{km} + g_m \gamma_{lm} \end{aligned} \tag{37}$$

with the initial conditions $\alpha(0)=1$, $\beta_k(0)=0$, and $\gamma_{kl}(0)=0$.

The physical observable of interest is again the time-dependent boson number which can be expressed in terms of the amplitudes $\alpha(t)$, $\beta_j(t)$, and $\gamma_{ij}(t)$ as

$$\langle n(t)\rangle = 3|\alpha(t)|^2 + 2\sum_j |\beta_j(t)|^2 + \sum_j |\gamma_{ij}(t)|^2. \quad (38)$$

Unlike before for $p=1$, the classical equations of motion Eqs. (7) and (8) and the Schrödinger Eqs. (35) and (37) are not equivalent in the subspaces of $p=2,3$. Solving these equations numerically, we compare the time-dependent boson number, given by Eqs. (11) and (38), for $p=2,3$ with the square modulus of the classical field $a(t)$ obtained from Eqs. (7) and (8). In the large-N limit, the solutions of both classical and quantum equations have exactly the same form in all regimes of the parameters including the intermediate regime of partial decay with a complex decay law.

As the classical and quantum solutions coincide in all regimes, the classical equations can be used to find the time dynamics of the boson occupation number. This is quite remarkable since the classical equations are significantly simpler to solve than the Schrödinger equation, both analytically and numerically. When the number of excitation is small, $p \ll N$, the classical equations can be mapped to the Schrödinger equation in the one-excitation subspace $p=1$ in leading $1/N$ order, see Eqs. (7) and (8). The Schrödinger equation for this case was already solved. A larger number p of excitations changes only the initial condition of Eq. (3) from $\alpha(0)=1$ to $\alpha(0)=\sqrt{p}$. This difference can be accounted for by a simple rescaling by p of the bosonic occupation number $\langle n(t)\rangle$ that was obtained in the single-excitation subspace for all regimes.

In conclusion, the analysis in Ref. 17 is also applicable to the case with more than one excitation, provided $p \ll N$ and $N \gg 1$.

VII. APPLICABILITY OF THE CLASSICAL APPROXIMATION

The classical approximation in the few-excitation sector is exact when the number of spins N is infinite. For finite but still large N's, i.e., $N \gg 1$, the time evolution of the classical system deviates from the quantum system by a small amount. The goal of this section is to analyze these finite-size deviations.[24]

A. Ehrenfest time

One way to quantify the difference between the classical and the quantum solution is to identify the Ehrenfest time τ_E at which they deviate significantly from each other. To this end, we compare the boson number $\langle n(t)\rangle$, obtained from the classical equations (in the few-excitation approximation), Eqs. (7) and (8), with the exact quantum solution in the two-excitation subspace obtained in Sec. V The solution to the classical equations Eq. (5) in this regime is $n=2\cos^2(\Omega t)$, where $\Omega=\sqrt{N\langle g^2\rangle}$. From Eq. (30), the solution to the Schrödinger equation is $\langle n\rangle = 2\cos^2(s_0 t/2)$ in leading $1/N$ order. Both solutions are single harmonic modes with frequencies that also match in leading $1/N$ order, where $s_0 = 2\sqrt{N\langle g^2\rangle}$. In first subleading $1/N$ order, the correction to s_0 depends explicitly on $Q_1(g)$, see Eqs. (19) and (20). For $\xi=0$, the expansion of Eq. (20) gives $s_0 = 2\sqrt{N\langle g^2\rangle} - \sqrt{4\langle g^2\rangle/N}$, and for $\xi=g_0$ expanding Eq. (19) we get $s_0 = 2\sqrt{N\langle g^2\rangle} - 3\sqrt{3\langle g^2\rangle/10N}$. Thus, at the time scale

$$\tau_E = \sqrt{\frac{N}{\langle g^2\rangle}}, \quad (39)$$

the phase difference between the two harmonic modes, with frequencies Ω and $s_0/2$, is comparable to 2π. Hence, the difference between classical and quantum solutions is significant for any value of ξ at this time scale τ_E, to which we refer as Ehrenfest time. The numerical prefactor depends on the particular type of inhomogeneity. The explicit calculations in Sec. V for typical distribution functions show that these numerical prefactors are of order 1.

There is also a $1/N$ correction to the amplitude of $\langle n(t)\rangle$ coming from the Schrödinger equation, see Eq. (32). This correction contains a decaying contribution [proportional to $I(t)$ given in Eq. (27)] which, again, marks a qualitative difference between the quantum and classical time dynamics in the two-excitation subspace. In particular, $I(t)$ decays at the characteristic time scale τ_g given in Eq. (28) which is equal to the Ehrenfest time τ_E introduced above. Thus, we see that this difference in the amplitude (although it is only a $1/N$ correction) is another manifestation of the quantum nature of the system where the time dynamics for times exceeding the Ehrenfest time can be described correctly only by the Schrödinger equation (and not by the classical one).

So far we have been using the approximate classical Eqs. (7) and (8) for few excitations, thereby neglecting the deviations of the z component of the classical spins from $C_j^z=-1/2$. To estimate the quality of this approximation, we use the result obtained in Ref. 25 for the homogeneous classical system. The solution of the unapproximated classical equations with $g_j \equiv g_0$ and $\epsilon_j \equiv \omega$ is an elliptic function of time.[25] When the number of excitations is small, $p \ll N$, this elliptic function can be expanded into a harmonic series with a leading term that reproduces the solution of the approximate Eqs. (7) and (8). The frequency of the leading harmonic term matches the frequency $\Omega=\sqrt{N}g_0$ from Eq. (5) in leading $1/N$ order but it also contains corrections on the order of $g_0/\sqrt{N}$ such as Eq. (30). Such corrections, however, are irrelevant as they become only sizable at the Ehrenfest time τ_E—the time beyond which the classical solution fails and the true time dynamics must be described anyway by the Schrödinger equation.

B. Initial spin excitations

Up to now, we have focused on a particular initial condition with excitations being initially present only in the boson mode. In contrast, a different initial condition was considered in Ref. 16, whereby the dynamics starts from an initial state with no boson present but, say, with the ith spin excited. Considering homogeneous systems, it was found that during the time evolution this ith spin remains excited if the total number of spins is large, regardless of how strong the spin-boson coupling is. The corresponding expectation value is

$\langle 0, \Downarrow \uparrow_i | S_i^z(t) | 0, \Downarrow \uparrow_i \rangle = 1/2 - [1 - \cos(\Omega t)]/N$. This result was associated with the effect of "radiation trapping," and it can also be obtained with the classical approximation. The corresponding initial condition $\mathbf{C}_{j\neq i}(0) = (0,0,-1/2)$, $\mathbf{C}_i(0) = (0,0,1/2)$, and $a(0)=0$ is a fixed point of the classical equations. Indeed, the effective magnetic field for each spin $\mathbf{B}_j = (0,0,\epsilon_j - \omega)$ has only a z component, and therefore the vector product of two parallel vectors vanishes, i.e., $\mathbf{B}_j \times \mathbf{C}_j = 0$. The dynamics of the classical field a is frozen as $C_j^- = 0$. Quantum corrections to this result show up only in the first $1/N$ correction. Thus, the classical approximation is also valid for a different initial condition in the few-excitation regime.

VIII. CONCLUSIONS

In this paper, we have shown that the solution to the classical Hamilton equations of motion of the inhomogeneous Dicke model coincide with the solution of the time-dependent Schrödinger equation when the number of spins N is large and the number of excitations p is small, $p \ll N$. For a single excitation, the leading $1/N$ order of the classical solution coincides with the quantum solution. For a few excitations such correspondence does not hold but for $p=2,3$ excitations, the numerical solutions of both classical equations of motion and Schrödinger equation coincide when the number of spins is large. It is plausible to conjecture that the same correspondence holds for $p>3$ in leading $1/N$ order.

To assess the validity of the classical approximation for $p>1$ excitations, we have solved the Schrödinger equation exactly in the two-excitation subspace with inhomogeneous coupling constants only and compared the result with the classical solutions. For large N, we performed an $1/N$ expansion of the solution to the Schrödinger equation and recovered the classical solution in leading order. Subleading $1/N$ corrections cause small deviations of the classical from the quantum solution, that, at a large time scale, make the difference between the two significant. This defines the Ehrenfest time that we identify in the limit of $p \ll N$ as $\tau_E = \sqrt{N/\langle g^2 \rangle}$.

Analyzing the solution to the Schrödinger equation for $p=2$, we compared it with the solutions to the Schrödinger equation for $p=1$. We have found that the boson occupation number in the two-excitation subspace exhibits a multifrequency dynamics due to the inhomogeneous couplings only, which, unlike in the single-excitation subspace, can lead to a decay in the limit of large N. But the leading term of an $1/N$ expansion recovers the single-frequency dynamics. The decay due to the inhomogeneity shows up only in the first subleading $1/N$ correction. We find that this contribution is an oscillatory mode with frequency $\frac{3}{2}\Omega$ and a slow decay envelope. The decay is essentially nonexponential with a long power-law tail, and the decay time is $\tau_g \sim \sqrt{N/\langle g^2 \rangle}$, where $\sqrt{\langle g^2 \rangle}$ is a characteristic coupling, the numerical prefactor is of order 1 for the special case of uniformly distributed coupling constants.

The decay due to an inhomogeneous coupling to a spin bath, which is unavoidable as the spins are located at different positions of the cavity mode (with different amplitudes of the electromagnetic field), is similar to the decay of an electron spin coupled to a bath of nuclear spins through the hyperfine interaction.[26,27] In the dynamics of a cavity mode, this mechanism can be neglected when only a few excitations are present in the system (for instance, in the few-photon spectroscopy experiments in Ref. 1) but may lead to a significant decay in a system with many excitations present initially (such as, for instance, in a bath of nuclear spins coupled to a cavity).

ACKNOWLEDGMENTS

We thank J. von Delft and A. Imamoglu for discussions. We acknowledge support from the Swiss NSF, NCCR Nanoscience Basel, JST ICORP, and DARPA QuIST.

APPENDIX: $1/N$ CORRECTIONS TO $\alpha_p(t)$ AND $\beta_k^p(t)$

In this appendix, we calculate the first $1/N$ correction to the pole contributions to the inverse Laplace transform of $\alpha(t)$ and $\beta_k(t)$ from Sec. V

If $\xi=0$, i.e., for homogeneous coupling constants, the solution to Eq. (12) simplifies. Substituting $g_j = g_0$ into Eqs. (14) and (15), we get

$$\beta_k(s) = \frac{i\sqrt{2}g_0}{s^2 + (4N-2)g_0^2} \tag{A1}$$

and

$$\alpha(s) = \frac{1}{s}\frac{s^2 + (2N-2)g_0^2}{s^2 + (4N-2)g_0^2}. \tag{A2}$$

These expressions have only poles but no branch points: two poles for $\beta_k(s)$, $s = \pm i 2 g_0 \sqrt{N - \frac{1}{2}}$ and three for $\alpha(s)$, $s = 0, \pm i 2 g_0 \sqrt{N - \frac{1}{2}}$, see Fig. 2. The inverse Laplace transform is given by residues only, $\alpha(t) = \alpha_p(t)$ and $\beta_k(t) = \beta_k^p(t)$,

$$\beta_k^p(t) = \frac{i \sin\left(2g_0\sqrt{N - \frac{1}{2}}t\right)}{\sqrt{2N-1}} \tag{A3}$$

and

$$\alpha_p(t) = \frac{N-1}{2N-1} + \frac{N}{2N-1}\cos\left(2g_0\sqrt{N-\frac{1}{2}}t\right). \tag{A4}$$

Expanding the above expression in $1/N$, we obtain the corrections $\delta\alpha(0)$ and $\delta\beta_k(0)$ in Eqs. (21) and (24). These corrections can also be obtained expanding the exactly solvable dynamics of homogeneous Dicke model.[28]

To calculate the $1/N$ correction when $\xi = g_0$, i.e., for maximum inhomogeneity, we expand Eq. (18) up to the second order in $1/N$ at the poles, $s = \pm i s_0$, $s_0 = \sqrt{4N\langle g^2 \rangle}$, and also account for the second-order corrections that come from the positions of the poles, $s_0 = \sqrt{4N\langle g^2 \rangle - \frac{6}{5}g_0^2}$.

Performing this procedure, we write the residues of $\alpha(s)$ at $s = \pm i s_0$ as

$$\mathrm{Res}_{s=\pm i s_0}\, \alpha(s) e^{st} = \frac{1}{\pm i s_0}\frac{N_0 + \delta N}{D_0 + \delta D} e^{\pm i s_0 t}, \tag{A5}$$

where

$$D_0 = -\frac{2(\pm is_0)Ng_0^2}{(-s_0^2+N\langle g^2\rangle)^2}, \tag{A6}$$

$$N_0 = 1+\frac{Ng_0^2}{3(-s_0^2+N\langle g^2\rangle)} \tag{A7}$$

are the denominator and numerator obtained using just $s_0=\sqrt{4N\langle g^2\rangle}$. Further,

$$\delta D = -\frac{2(\pm is_0)Ng_0^2}{(-s_0^2+N\langle g^2\rangle)^2}\frac{12g_0^2}{5(-s_0^2+N\langle g^2\rangle)}, \tag{A8}$$

$$\delta N = \frac{2Ng_0^4}{5(-s_0^2+N\langle g^2\rangle)^2} \tag{A9}$$

are the first $1/N$ corrections. The average $\langle g^2\rangle = g_0^2/3$ is evaluated using $Q_1(g)$ with $\xi=g_0$.

Performing the summation over the two poles $\pm is_0$, we get

$$\sum_{\pm is_0}\mathrm{Res}_{s=\pm is_0}\,\alpha(s)e^{st} = \frac{2}{is_0}\frac{N_0+\delta N}{D_0+\delta D}\cos(s_0t) \tag{A10}$$

and expand it in the small parameter as

$$\sum_{\pm is_0}\mathrm{Res}_{s=\pm is_0}\,\alpha(s)e^{st} = \frac{2}{is_0}\frac{N_0}{D_0}\left(1+\frac{\delta N}{N_0}\right)\left(1-\frac{\delta D}{D_0}\right)\cos(s_0t), \tag{A11}$$

where the first two terms in the product still have to be expanded in the small correction to $s_0=\sqrt{4N\langle g^2\rangle}$, and the last two have to be calculated using only the leading term $s_0=\sqrt{4N\langle g^2\rangle}$.

The first two terms, which have to be calculated with $s_0=\sqrt{4N\langle g^2\rangle-\frac{6}{5}g_0^2}$, are

$$\begin{aligned}\frac{2}{is_0}\frac{N_0}{D_0} &= \frac{2}{i\sqrt{4N\langle g^2\rangle}}\left(1+\frac{3g_0^2}{20N\langle g^2\rangle}\right)\left(\frac{2}{3}-\frac{2}{5N}\right)\\ &\times\frac{-g_0^2N}{i2\sqrt{4\langle g^2\rangle}}\left(1-\frac{3}{5N}\right)\left(1+\frac{9}{20N}\right)\\ &\approx\frac{1}{2}\left(1+\frac{9}{10N}\right)\left(1-\frac{6}{5N}\right)\approx\frac{1}{2}\left(1-\frac{3}{10N}\right)\end{aligned} \tag{A12}$$

and the last two, which have to be calculated with $s_0=\sqrt{4N\langle g^2\rangle}$, are

$$\left(1+\frac{\delta N}{N_0}\right)\left(1-\frac{\delta D}{D_0}\right)=\left(1+\frac{3}{5N}\right)\left(1+\frac{12}{5N}\right)\approx 1+\frac{3}{N}. \tag{A13}$$

Finally, the contribution from the poles $\pm is_0$ is

$$\sum_{\pm is_0}\mathrm{Res}_{s=\pm is_0}\,\alpha e^{st} = \frac{1}{2}\cos(s_0t)+\frac{27}{20N}\cos(s_0t). \tag{A14}$$

The residue of $\alpha(s)$ at $s=0$ is also expanded in the small corrections,

$$\mathrm{Res}_{s=0}\,\alpha(s) = \frac{N_0+\delta N}{D_0+\delta D}\approx\frac{N_0}{D_0}\left(1+\frac{\delta N}{N_0}\right)\left(1-\frac{\delta D}{D_0}\right), \tag{A15}$$

where

$$\frac{\delta N}{N_0}=\frac{9}{5N},\quad \frac{\delta D}{D_0}=\frac{36}{5N}. \tag{A16}$$

And the contribution from the pole $s=0$ is

$$\mathrm{Res}_{s=0}\,\alpha(s) = \frac{1}{2}-\frac{27}{20N}. \tag{A17}$$

The sum of Eqs. (A14) and (A17) gives the correction $\delta\alpha(g_0)$ from Eq. (21).

Then, we calculate the corrections to $\beta_k^p(t)=\mathrm{Res}_{s=\pm is_0}\,\beta_k(s)e^{st}$. Expanding the residues at $s=\pm is_0$, where $s_0=\sqrt{4N\langle g^2\rangle-\frac{6}{5}g_0^2}$, we get

$$\begin{aligned}\mathrm{Res}_{s=\pm is_0}\,\beta_k(s)e^{st} &= \frac{-i\sqrt{2}g_ke^{\pm is_0t}}{s_0^2-N\langle g^2\rangle+2g_k^2}\frac{1}{D_0+\delta D}\\ &\approx\frac{-i\sqrt{2}g_ke^{\pm is_0t}}{s_0^2-N\langle g^2\rangle+2g_k^2}\frac{1}{D_0}\left(1-\frac{\delta D}{D_0}\right),\end{aligned} \tag{A18}$$

where D_0 and δD have already been calculated, see Eqs. (A6) and (A8). Similarly to the calculation of $\alpha(s)$, we again expand and get

$$\begin{aligned}\mathrm{Res}_{s=\pm is_0}\,\beta_k(s)e^{st} &= \frac{-i\sqrt{2}g_k}{Ng_0^2}\left(1-\frac{2(g_k/g_0)^2}{N}+\frac{6}{5N}\right)\\ &\times\frac{Ng_0^2}{(\pm i)4\sqrt{N\langle g^2\rangle}}\left(1-\frac{3}{5N}\right)\\ &\times\left(1+\frac{12}{5N}\right)e^{\pm is_0t}.\end{aligned} \tag{A19}$$

The sum over these residues,

$$\begin{aligned}\beta_k^p(g_0) &= \frac{ig_k\sqrt{2}}{2\sqrt{N\langle g^2\rangle}}\left(1-\frac{2(g_k/g_0)^2}{N}+\frac{6}{5N}\right)\left(1+\frac{9}{5N}\right)\sin(s_0t)\\ &\approx\frac{ig_k}{\sqrt{2N\langle g^2\rangle}}\left(1-\frac{2(g_k/g_0)^2}{N}+\frac{3}{N}\right)\sin(s_0t)\end{aligned} \tag{A20}$$

is the correction from Eq. (24) for $\xi=g_0$.

[1] F. Brennecke, T. Donner, S. Ritter, T. Bourdel, M. Kohl, and T. Esslinger, Nature (London) **450**, 268 (2007).
[2] J. Kasprzak, M. Richard S. Kundermann, A. Baas, P. Jeambrun, J. M. J. Keeling, F. M. Marchetti, M. H. Szymańska, R. André, J. L. Staehli, V. Savona, P. B. Littlewood, B. Deveaud, and L. S. Dang, Nature (London) **443**, 409 (2006).
[3] T. B. Norris, J.-K. Rhee, C.-Y. Sung, Y. Arakawa, M. Nishioka, and C. Weisbuch, Phys. Rev. B **50**, 14663 (1994).
[4] R. H. Dicke, Phys. Rev. **93**, 99 (1954).
[5] J. I. Cirac and P. Zoller, Phys. Rev. Lett. **74**, 4091 (1995).
[6] A. Imamoglu, D. D. Awschalom, G. Burkard, D. P. DiVincenzo, D. Loss, M. Sherwin, and A. Small, Phys. Rev. Lett. **83**, 4204 (1999).
[7] L. Childress, A. S. Sørensen, and M. D. Lukin, Phys. Rev. A **69**, 042302 (2004).
[8] M. Trif, V. N. Golovach, and D. Loss, Phys. Rev. B **77**, 045434 (2008).
[9] A. Imamoglu, Phys. Rev. Lett. **102**, 083602 (2009).
[10] R. J. Thompson, G. Rempe, and H. J. Kimble, Phys. Rev. Lett. **68**, 1132 (1992).
[11] J. I. Cirac, P. Zoller, H. J. Kimble, and H. Mabuchi, Phys. Rev. Lett. **78**, 3221 (1997).
[12] D. L. Huffaker, G. Park, Z. Zou, O. B. Shchekin, and D. G. Deppe, Appl. Phys. Lett. **73**, 2564 (1998).
[13] C. Schneider, T. Heindel, A. Huggenberger, P. Weinmann, C. Kistner, M. Kamp, S. Reitzenstein, S. Hafling, and A. Forchel, Appl. Phys. Lett. **94**, 111111 (2009).
[14] M. Sugawara, N. Hatori, M. Ishida, H. Ebe, Y. Arakawa, T. Akiyama, K. Otsubo, T. Yamamoto, and Y. Nakata, J. Phys. D **38**, 2126 (2005).
[15] M. Tavis and F. W. Cummings, Phys. Rev. **170**, 379 (1968).
[16] F. W. Cummings and A. Dorri, Phys. Rev. A **28**, 2282 (1983).
[17] O. Tsyplyatyev and D. Loss, Phys. Rev. A **80**, 023803 (2009).
[18] C. E. López, H. Christ, J. C. Retamal, and E. Solano, Phys. Rev. A **75**, 033818 (2007).
[19] R. Bonifacio, P. Schwendimann, and F. Haake, Phys. Rev. A **4**, 854 (1971).
[20] F. Deppe, M. Mariantoni, E. P. Menzel, A. Marx, S. Saito, K. Kakuyanagi, H. Tanaka, T. Meno, K. Semba, H. Takayanagi, E. Solano, and R. Gross, Nat. Phys. **4**, 686 (2008).
[21] J. Jacobson, S. Pau, H. Cao, G. Björk, and Y. Yamamoto, Phys. Rev. A **51**, 2542 (1995).
[22] A. V. Andreev, V. Gurarie, and L. Radzihovsky, Phys. Rev. Lett. **93**, 130402 (2004).
[23] P. R. Eastham and P. B. Littlewood, Phys. Rev. B **64**, 235101 (2001).
[24] In a diffusive system, the Ehrenfest time is the time scale at which a minimal wave packet spreads over a characteristic spatial scale (Refs. 29–31).
[25] E. T. Jaynes and F. W. Cummings, Proc. IEEE **51**, 89 (1963).
[26] A. V. Khaetskii, D. Loss, and L. Glazman, Phys. Rev. Lett. **88**, 186802 (2002).
[27] W. A. Coish and D. Loss, Phys. Rev. B **70**, 195340 (2004).
[28] Y. Yamamoto and A. Imamoglu, *Mesoscopic Quantum Optics* (Willey, New York, 1999).
[29] I. L. Aleiner and A. I. Larkin, Phys. Rev. B **54**, 14423 (1996).
[30] I. Adagideli and C. W. J. Beenakker, Phys. Rev. Lett. **89**, 237002 (2002).
[31] S. Rahav and P. W. Brouwer, Phys. Rev. Lett. **95**, 056806 (2005).